EFDA–JET–CP(10)08/10

T. Tala, Y. Lin, P. Mantica, M.F.F. Nave, Y. Sun, T.W. Versloot, P.C. de Vries, C.Angioni, O. Asunta, G. Corrigan, C. Giroud, J. Ferreira, T. Hellsten, T. Johnson, H. Koslowski, E. Lerche, Y. Liang, J. Lönnroth, V. Naulin, A.G. Peeters, J.E. Rice, A. Salmi, W. Solomon, D. Strintzi, G. Tardini, M. Tsalas, D. van Eester, J. Weiland, H. Weisen, K.-D. Zastrow and JET EFDA contributors

JET Rotation Experiments Towards the Capability to Predict the Toroidal Rotation Profile

JET Rotation Experiments Towards the Capability to Predict the Toroidal Rotation Profile

T. Tala[1], Y. Lin[2], P. Mantica[3], M.F.F. Nave[4], Y. Sun[5], T.W. Versloot[6], P.C. de Vries[6], C. Angioni[7], O. Asunta[8], G. Corrigan[9], C. Giroud[9], J. Ferreira[4], T. Hellsten[10], T. Johnson[10], H. Koslowski[5], E. Lerche[11], Y. Liang[5], J. Lönnroth[8], V. Naulin[12], A.G. Peeters[13], J.E. Rice[2], A. Salmi[1], W. Solomon[14], D. Strintzi[15], G. Tardini[5], M. Tsalas[15,18], D. van Eester[11], J. Weiland[16], H. Weisen[17,18], K.-D. Zastrow[9] and JET EFDA contributors*

JET-EFDA, Culham Science Centre, OX14 3DB, Abingdon, UK

[1]Association EURATOM-Tekes, VTT, P.O. Box 1000, FIN-02044 VTT, Finland
[2]MIT Plasma Science and Fusion Center, Cambridge, MA, USA
[3]Istituto di Fisica del Plasma CNR-EURATOM, via Cozzi 53, 20125 Milano, Italy
[4]Associação EURATOM/IST, Instituto de Plasmas e Fusao Nuclear, 1049-001 Lisbon, Portugal
[5]Institute for Energy Research – Plasma Physics, Forschungszentrum Jülich, Association EURATOMFZJ, Trilateral Euregio Cluster, 52425 Jülich, Germany
[6]FOM Institute Rijnhuizen, Association EURATOM-FOM, Nieuwegein, the Netherlands
[7]Max-Planc-Iinstitut für Plasmaphysik, EURATOM-Assoziation, Garching, Germany
[8]Association EURATOM-Tekes, Aalto University, Department of Applied Physics, Finland
[9]EURATOM/CCFE Fusion Association, Culham Science Centre, OX14 3DB, Abingdon, OXON, UK
[10]Association EURATOM-VR, Fusion Plasma Physics, EES, KTH, Stockholm, Sweden
[11]LPP-ERM/KMS, Association Euratom-Belgian State, TEC, B-1000 Brussels, Belgium
[12]Association Euratom-Risø-DTU, Denmark
[13]Center for Fusion, Space and Astrophysics, Department of Physics, Univ. of Warwick, UK
[14]Princeton Plasma Physics Laboratory, Princeton University, Princeton, New Jersey 08543, USA
[15]Association EURATOM Hellenic Republic, Athens, Greece
[16]Association EURATOM-VR, Chalmers University of Technology, Göteborg, Sweden
[17]Association EURATOM-Confédération Suisse, EPFL, CRPP, CH-1015 Lausanne, Switzerland
[18]EFDA-CSU, Culham Science Centre, OX14 3DB, Abingdon, OXON, UK
** See annex of F. Romanelli et al, "Overview of JET Results", (23rd IAEA Fusion Energy Conference, Daejon, Republic of Korea (2010)).*

Preprint of Paper to be submitted for publication in Proceedings of the 23rd IAEA Fusion Energy Conference, Daejon, Republic of Korea (10th October 2010 - 16th October 2010)

ABSTRACT

The existence of an inward momentum pinch in JET plasmas was reported in the last IAEA meeting. Since then, several parametric scans to study the size of the inward momentum pinch demonstrate very robustly that the pinch number Rv_{pinch}/χ_ϕ in H-mode plasmas is between $3-5$ at $r/a = 0.4-0.8$. Only in plasmas with $R/Ln > 3$, larger $Rv_{pinch}/\chi_\phi > 5$ are found while other parametric dependencies are weaker. The Prandtl number is not found to depend very strongly on any of the parameters scanned, the values being typically between 1.5 and 2 at mid-radius. In intrinsic rotation studies, toroidal magnetic field ripple was found to affect both the edge rotation by lowering it typically close to zero or to small counter-rotation values and also core rotation where it is counter-rotating. An experiment to study Mode Conversion Flow Drive was performed using He^3 ICRH scheme. Large central counter-rotation up to $v_\phi = -30$km/s was observed at He^3 concentration levels of 10-17%, the rotation being proportional to ICRH power. A strong toroidal rotation braking has been observed in plasmas with application of an n=1 magnetic perturbation field. The inferred torque has a global profile and originates from non-resonant components. Two types of edge rotation sinks have been analysed using recent JET data. Firstly, ELMs have been found to consistently cause a larger drop in momentum in comparison with the energy loss. Secondly, a difference in the magnitude of momentum and energy losses created by multiple charge-exchange reactions between neutrals and ions is observed, and with a significantly larger reduction in momentum than in energy content. While it seems probable that rotation profiles will be peaked in ITER thanks to the robust pinch term, its absolute value is still very challenging to predict with the present knowledge of sources and sinks and also due to the uncertainties in the rotation around the plasma edge.

1. INTRODUCTION

Plasma rotation and momentum transport are currently very active areas of research, both experimentally and theoretically. It is well-known that sheared plasma rotation can stabilise turbulence while the rotation itself has beneficial effects on MHD modes, such as resistive wall modes or neo-classical tearing modes. Although the importance of rotation has been recently recognised, predicting or extrapolating the toroidal rotation profile has turned out to be extremely challenging and several key issues remain. This paper reports a significant progress recently in understanding both the areas of momentum transport and rotation sources and sinks. The topics also cover recent intrinsic rotation studies with different heating schemes and toroidal magnetic field ripple, ELMs and edge momentum losses and rotation braking studies with error field coils.

2. MOMENTUM TRANSPORT STUDIES

As reported in the last IAEA conference, an inward momentum pinch, in many cases very significant in size, has been found on JET [1,2,3,4]. In the present work, the parametric dependencies of the pinch on several key parameters are studied, in order to see whether a centrally peaked toroidal velocity profile can occur, for example in ITER, even in the absence of any central momentum

source. Experiments where the NBI power and torque were modulated have been performed on JET to infer both the inward pinch number (defined as Rv_{pinch}/χ_ϕ) and the Prandtl number profile.

The pinch number has been found to depend most strongly on R/L_n, a factor of 2 increase in R/L_n yielding roughly a factor of 1.5 increase in Rv_{pinch}/χ_ϕ, as illustrated in figure 1 (left frame). The dependence of Rv_{pinch}/χ_ϕ on q was much smaller and partly masked by the changing R/L_n when scanning the q. A dedicated collisionality scan was carried out by keeping all the other dimensionless parameters constant. Neither Rv_{pinch}/χ_ϕ nor P_r depended on collisionality significantly. The Prandtl number did not depend either on R/Ln (figure 1, right frame), q or the line average density. Low power L-mode plasmas tend to have Prandtl numbers typically about 20% higher than those in H-mode. There is a strong radial dependence for both the pinch and in particular for the Prandtl numbers, typically an increase of a factor 1.5 or larger occurring when going from $r/a = 0.3$ to $r/a = 0.8$.

The observed trends in the parametric scans with linear gyro-kinetic momentum transport simulations using GKW [5] and GS2 [6] are in a quantitative agreement with experimental trend with respect to R/L_n dependence. In addition, consistently with experiments, the gyrokinetic simulations do not find any clear collisionality dependence for neither pinch nor Prandtl numbers. The radially increasing Prandtl numbers are also reproduced well in the simulations. While the simulated parametric and radial trends agree even quantitatively with the experimental ones, the simulated values of both Rv_{pinch}/χ_ϕ and P_r are, however, significantly lower than the experimental ones, in most cases by a factor of 1.5–2.

Another tool to study core momentum transport is to vary edge toroidal rotation by increasing toroidal magnetic ripple. At ripple values of 1% or higher, the edge rotation at $r/a = 0.9$ becomes close to zero or even negative. In these plasmas, the rotation profile is much less peaked although the core torque sources are the same. This indicates clearly the existence of the momentum pinch in a wide range of JET plasmas, as the effect of momentum pinch on the rotation value itself becomes smaller at low (edge) rotation [7]. Furthermore, according to JET momentum database studies, Rv_{pinch}/χ_ϕ was found be larger in plasmas with higher R/L_n, consistent with the NBI modulation studies reported above [7,8].

3. INTRINSIC ROTATION IN JET EXPERIMENTS WITH DIFFERENT ICRH SCHEMES

The following three different types of experiments were performed to study intrinsic rotation in ICRH heated and Ohmic plasmas: intrinsic rotation with toroidal magnetic ripple, intrinsic rotation in H-mode plasmas and the flow drive by ICRH mode conversion with He^3.

3.1. EFFECT OF MAGNETIC RIPPLE ON INTRINSIC ROTATION

Using the unique capability of JET to monotonically change the amplitude of the magnetic field ripple, without modifying other relevant equilibrium conditions, the effect of the ripple on the

angular rotation frequency of the plasma column was investigated under the conditions of no external momentum input [9,10]. The ripple amplitude was varied from $\delta = 0.08\%$ to $\delta = 1.5\%$ in Ohmic and ICRH heated plasmas. In plasmas with the usual JET ripple of $\delta = 0.08\%$, the intrinsic rotation frequency level is always smaller than $\omega_\phi < \pm 10$ krad/s [11]. Furthermore, the edge is always co-rotating while the core can be either counter- or corotating depending on the plasma current, the rotation usually increasing in co-direction with increasing Ip.

Ripple affects both the edge rotation by lowering it typically close to zero or to small counterrotation values and also core rotation where it becomes counter-rotating as illustrated in figure 2 (left frame). It also shows that there is a clear difference between type I and III ELMs; core counter-rotation was observed to be larger in phases with type III ELMs. However, it is not yet clear if this is a pedestal, density or collisionality effect. In these plasmas, the magnetic axis is at $R_0 = 3.02$m, and the ICRH resonance location is slightly off-axis on the high-field side at $R_{res} = 2.71$m. Furthermore, the largest edge and core counter rotation was observed when the ICRH resonance location is on the low-field side, where the ripple amplitude is larger, as shown in figure 2 (right frame). This correlation between the magnitude of intrinsic rotation and ICRH resonance position indicates that the interaction between fast ions and ripple creates torque in the counter rotation.

Both in the case of plasmas with no momentum input (ICRH) and then even without any fast ions (Ohmic), increasing ripple was found to cause counter rotation [9]. This indicates a strong torque due to non-ambipolar transport of thermal ions and in the case of ICRH also fast ions as the central rotation was significantly modified due to ripple. It is also clear that the effect of ripple on rotation originates from different physics in ICRH and Ohmic plasmas in experiments NBI heating. In the latter case, ripple reduced rotation is mainly located at the edge region [12], originating dominantly from the torque caused by the ripple lost fast NBI ions [13]. Recently, the NBI torque calculation with ripple in the ASCOT code [14] has been successfully benchmarked against NBI modulation, showing consistency with experimental results.

3.2. INTRINSIC ROTATION IN H-MODE PLASMAS ON JET

Intrinsic rotation experiments with large ICRH power leading to H-mode at $\beta \approx 1.3$ shows that the plasma rotation is still very close to zero on JET. The new data are in contradiction with Rice scaling law [15] that extrapolates to roughly 10 times higher Mach Alfven number $MA = V_\phi / V_A$ (VA is Alfven velocity) at such β than observed on JET. Intrinsic rotation experiments with even higher β on JET will be useful understand how the rotation extrapolates to ITER.

3.3. ICRH MODE CONVERSION FLOW DRIVE EXPERIMENT

An experiment to study Mode Conversion Flow Drive (MCFD) was performed in L-mode plasmas at $B_t = 3.45$T with varying I_p using He^3 ICRH scheme. MCFD was found to be sensitive to He^3 concentration level as illustrated figure 3 (left frame). Large central counterrotation up to $\omega_\phi = -10$krad/s

($v_\phi = -30$ km/s) was observed at He^3 concentration levels of 10- 17% [16]. Normal intrinsic rotation levels (<10km/s) at $P_{ICRH} = 3$MW were recovered at low (<4%) and He^3 concentration level, i.e. with standard He^3 minority heating scheme (<4%) and also under pure mode conversion scheme (He^3 concentration level > 25%), although it is to be noted that the heating power is a bit lower there.

The amount of counter-rotation scales linearly with ICRH power. The largest counter-rotation around $\omega_\phi = -10$krad/s was obtained at low current $I_p = 1.8$MA while the higher $I_p = 2.8$MA discharges had central values typically around $\omega_\phi = -6$ krad/s. The driven rotation is peaked on-axis, but there is a clear effect at all radii, the edge co-rotation being dragged down practically to zero from the usual $\omega_\phi = 3-4$ krad/s level. The estimated MCFD torque also has a global profile as shown in figure 3 (right frame). The torque profile has been calculated from break-in-slope analysis of the ICRH power modulation. We have assumed here for simplicity that all the changes in rotation by modulation are due to the MCFD source, hence neglecting all the possible changes in transport, such as momentum diffusivity and pinch variations due to the power (temperature) modulation. Therefore, the torque profile can be considered as an upper estimate, being with this assumption as high as even 50% of the torque produced by the NBI system at the same power and a factor 4 higher than the direct momentum injection from the RF waves.

The physical mechanism of MCFD is not yet completely understood, but an up-down asymmetry in the mode conversion process and wave momentum redistribution has been proposed as a plausible candidate [17]. There, the MCFD power can be either deposited predominantly on upper or lower side or its radial deposition profile can be different on the upper and lower sides of the absorption layer. Even if the power deposition would have a dipole shape, the torque deposited on the outer radius would be transported faster out, thus producing a net momentum source. Many JET observations of MCFD, such as the rotation being counter-I_p and the He^3 concentration dependence, are consistent with the up-down asymmetry hypothesis. Same MCFD experiment in hydrogen plasma with He3 has also been performed on JET and similar amount of driven rotation was observed.

4. EXPERIMENTS TO STUDY ROTATION SOURCES AND SINKS

4.1 Toroidal Rotation Braking with n = 1 Magnetic Perturbation Field on JET

A strong toroidal rotation braking has been observed in plasmas with application of an n = 1 magnetic perturbation field on JET [18]. Inferred results from the momentum transport analysis show that the torque induced by the n = 1 perturbation field has a global profile, presented in figure 4 (left frame). The maximum value (typically about half of the NBI torque) of the torque is at the plasma central region ($\rho < 0.4$). Moreover, it is not localised at certain magnetic surfaces, indicating that the non-resonant component dominates over the resonant magnetic braking.

In the torque calculation procedure, the Polynomial functions are used as base functions for χ_ϕ and v_{pinch},

$$\chi_\phi = \sum_{n=0}^{N} \alpha_n \rho^n, \qquad v_{pinch} = \sum_{m=0}^{M} \beta_m \rho^m,$$

where α, β are the unknown free parameters to be fitted and N and M are the orders of the Polynomial base functions. It is to be noted that the obtained torque profile is not very sensitive to the selected set of base functions, making the torque profile a robust estimate. The obtained torque profile is mainly determined by the change of the total momentum flux due to the magnetic perturbation even if in these calculations the pinch velocities change on a large range (0−20 m/s).

The Neoclassical Toroidal Viscosity (NTV) calculation shows that these JET plasmas in the core region are in the $\sqrt{\nu}$ regime (ν regime with collisional boundary layer effect taken into account), but however, not very far from $1/\nu$ regime. Therefore, we also show the NTV torque for that regime. The calculated NTV torque profile in the $\sqrt{\nu}$ regime is an order of magnitude smaller than the experimentally observed torque profile T_{EFCC}, shown in figure 4 (right frame). On the other hand, T_{EFCC} is about four times smaller than NTV torque in the $1/\nu$ regime.

4.2. EFFECT OF ELMS AND NEUTRAL PARTICLES ON ROTATION IN JET H-MODE DISCHARGES

The loss of plasma toroidal angular momentum and thermal energy due to Edge Localized Modes (ELMs) has been studied in JET. The analysis shows a consistently larger drop in momentum in comparison with the energy loss associated with the ELMs, shown in figure 5 (left frame) [19], under a wide variety of plasma conditions. This difference originates firstly from the large reduction in angular frequency at the plasma edge, observed to penetrate deep into the plasma up to r/a = 0.65 during large type-I ELMs while the reduction in energy extends only to r/a = 0.8, and secondly, due to a longer build-up time for the momentum density at the plasma edge after the ELM crash. As a result, the time averaged angular frequency is lowered near the top of the pedestal with increasing ELM frequency more than the temperature drop, hence resulting in a significant drop in thermal Mach number at the edge.

Charge-Exchange interactions between the plasma ions and the neutral particle background create a continuous sink of momentum and energy. To quantify a difference in the magnitude of momentum and energy losses created by multiple charge-exchange reactions, a series of discharges was selected with a similar plasma configuration and equal external heating powers, but increasing input gas flux during the flat top of the H-mode period [20]. In figure 5 (right frame), thermal energy Wth and angular momentum L_φ of all discharges are shown normalised to the non-fuelled case. A clear decrease is observed as the confinement degrades but with a significantly larger reduction in L_φ. The magnitude of CX losses increases to approximately 10% of the total input torque with the power losses being smaller. Therefore, the amount and profile of neutrals, not known usually very accurately in tokamak plasmas, will affect the boundary value of rotation, making the rotation profile extrapolation even more challenging for future tokamaks.

CONCLUSIONS

Several parametric scans to study the size of the inward momentum pinch demonstrate robustly that

the pinch number Rv_{pinch}/χ_ϕ is between 3–5 at r/a = 0.4–0.8 for all plasma conditions scanned so far. Only in plasmas with $R/L_n > 3$, larger Rv_{pinch}/χ_ϕ are found while other parametric dependencies are weaker. The Prandtl number is found not to depend very strongly on any of the parameters scanned, the values being typically between 1.5 and 2 at mid-radius. Based on the results from these parametric scans of the pinch and Prandtl numbers, one can conclude that the rotation profile will be peaked in ITER provided that some rotation sources are available, even at the edge of the plasma, to make the plasma rotation be finite such that the inward pinch can be effective. However, in predicting the rotation values for ITER, much larger uncertainties remain because understanding of different type rotation of sources and sinks will crucial. In particular, braking effects from resonant magnetic perturbation and different types of rotation sources and sinks at the edge will give large uncertainties in any extrapolation of the rotation profile for future tokamaks. In conclusion, while it seems robust that the rotation profile will be peaked in ITER, the absolute magnitude of rotation remains still very challenging to predict with the present uncertainties in sources/sinks and boundary conditions.

ACKNOWLEDGEMENTS

This work was supported by EURATOM and carried out within the framework of the European Fusion Development Agreement. The views and opinions expressed herein do not necessarily reflect those of the European Commission.

REFERENCES

[1]. T. Tala et al., Physical Review Letters **102**, 075001 (2009).
[2]. T. Tala, et al., Plasma Physics and Controlled Fusion 49, B291 (2007).
[3]. P. Mantica et al., "Perturbative studies of toroidal momentum transport using NBI modulation in JET: experimental results, analysis methodology and first principle modelling", in press, Physics of Plasmas (2010).
[4]. G. Tardini et al., Nuclear Fusion **49**, 085010 (2009).
[5]. A.G. Peeters and D. Strintzi, Physics of Plasmas **11**, 3748 (2004).
[6]. W. Dorland, F. Jenko, M. Kotschenreuther, and B. N. Rogers, Physical Review Letters **85**, 5579 (2000).
[7]. P.C. de Vries et al., Plasma Physics and Controlled Fusion **52**, 065004 (2010).
[8]. H. Weisen et al.," Statistical evidence for non-diffusive momentum transport in JET neutral beam heated Hmode discharges", 15th EU-US Transport Task Force Meeting, Cordoba, Spain, 7–10 September 2010.
[9]. M.F.F. Nave et al., Physical Review Letters **105**, 105005 (2010).
[10]. M.F.F. Nave et al., ''Toroidal rotation in JET ICRF heated H-mode plasmas'', 37th EPS Conference on Plasma Physics, Dublin, Ireland, 21–25 June 2010.
[11]. L.-G. Eriksson et al., Plasma Physics and Controlled Fusion **51**, 044008 (2009).
[12]. P.C. de Vries et al., Nuclear Fusion **48**, 035007 (2008).

[13]. A. Salmi et al., Contribution Plasma Physics **48**, 77 (2008).
[14]. J.A. Heikkinen et al., Journal of Computational Physics **173**, 527 (2001).
[15]. J.E. Rice et al., Nuclear Fusion **47**, 1618 (2007).
[16]. Y. Lin et al., "ICRF mode conversion flow drive in JET D(^{3}He) plasmas and comparison with results from Alcator C-Mod", 37th EPS Conference on Plasma Physics , Dublin, Ireland, 21–25 June 2010.
[17]. Y. Lin et al., "ICRF mode conversion flow drive in D(^{3}He) plasmas on JET", to be submitted to Plasma Physics and Controlled Fusion.
[18]. Y. Sun et al., Plasma Phys. Control. Fusion **52**, 105007 (2010) and this conference, paper EXS/P3-06.
[19]. T. Versloot et al., Plasma Phys. Control. Fusion **52**, 045014 (2010).
[20]. T. Versloot et al., "Momentum Losses by Charge Exchange with Neutral Particles in H-mode Discharges at JET", 37th EPS Conference on Plasma Physics , Dublin, Ireland, 21–25 June 2010.

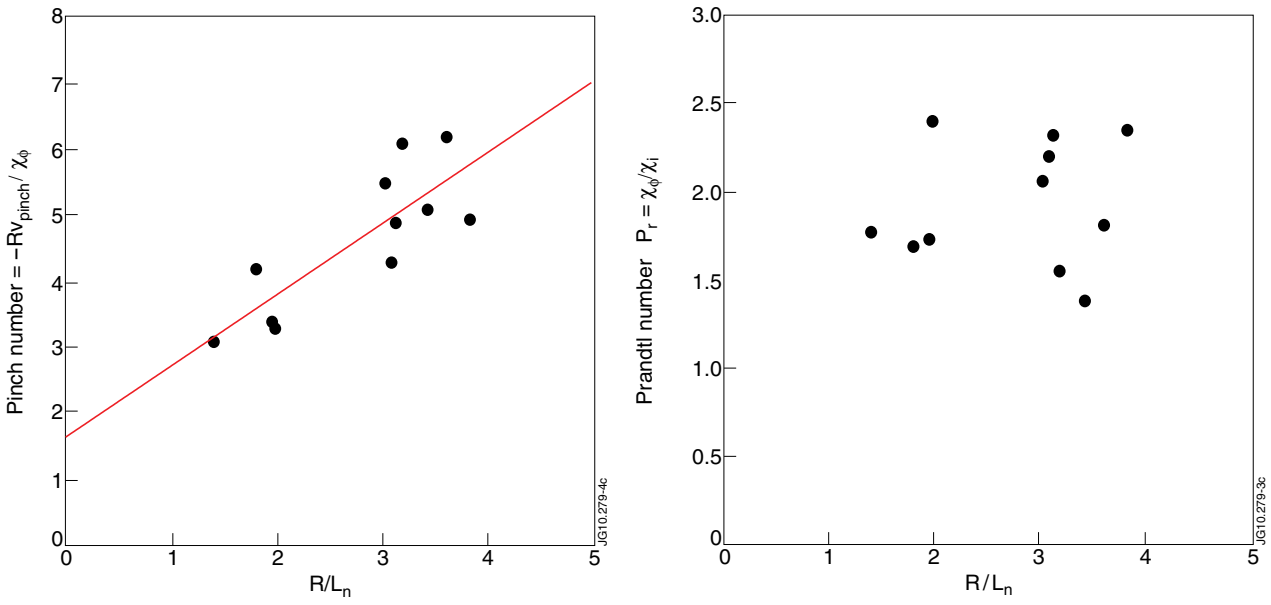

Figure 1: Dependence of $-Rv_{pinch}/\chi_\phi$ (left frame) and P_r (right frame) on R/L_n. All data are averaged over the radius from r/a = 0.4 to r/a = 0.8.

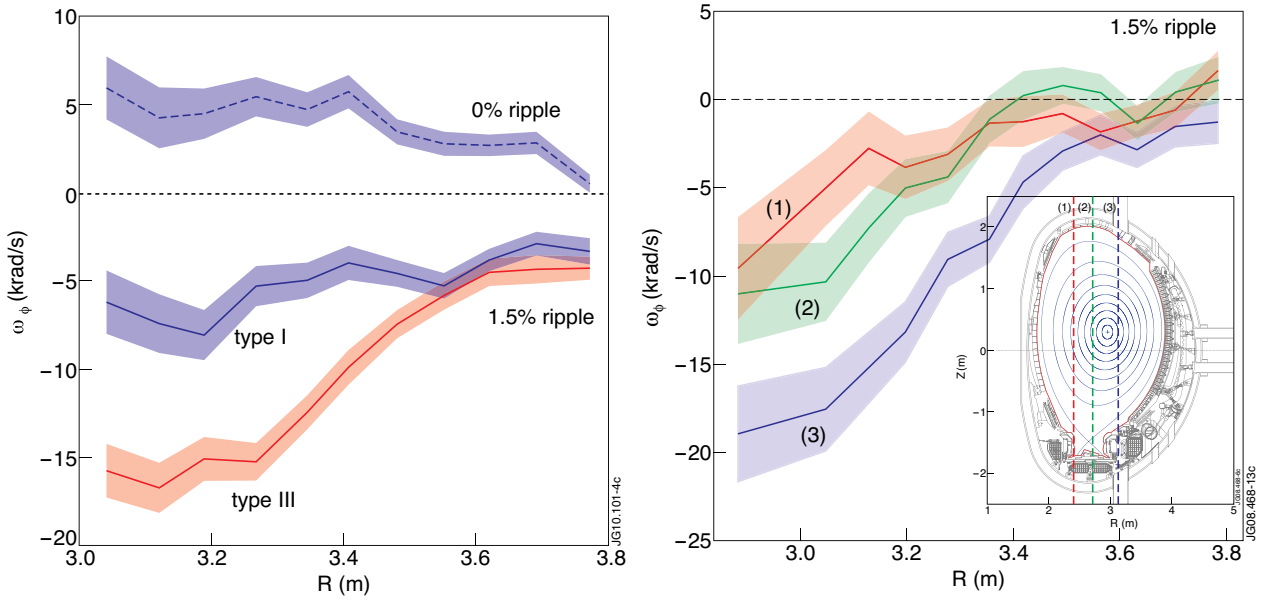

Figure 2: (Left frame) Toroidal angular rotation profiles for ICRF heated H-mode plasmas with I_p = 1.5MA, B_T = 2.2 T, P_{ICRH}=3 MW for the two ripple levels. Top Pulse No: (red curve) 74688 with δ = 0.08% and P_{ICRF} = 3.1MW; bottom pulse (green and blue curves) 74686 δ = 1.5% and P_{ICRF}= 2.9MW, including both the type I and type III ELM phase. (Right frame) Toroidal angular rotation profiles for L-mode pulses with δ = 1.5%, I_p = 1.5MA, P_{ICRH} = 2MW, for three different resonance positions: (1) 77010 with R_{res} = 2.38m, (2) 77014 with R_{res} = 2.71m, (3) Pulse No: 77009 with R_{res} = 3.13m. The resonance positions with respect to the magnetic axis R_0 = 2.95m are shown in the inset. Reprinted from [9,10].

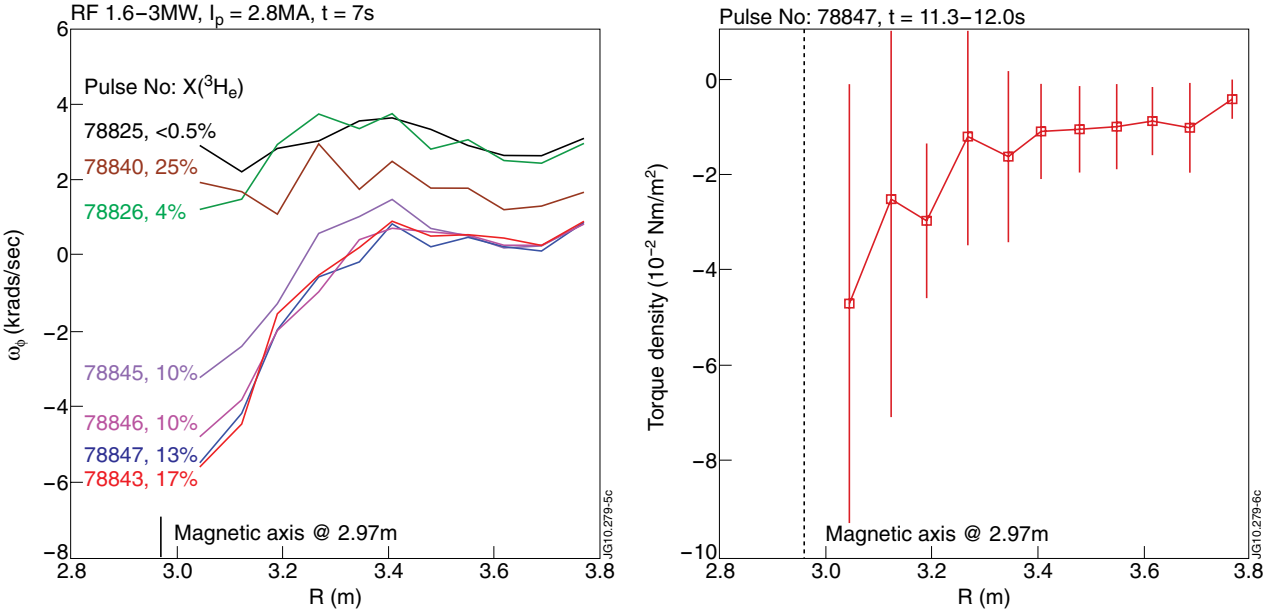

Figure 3: (Left frame) Toroidal rotation profiles from I_p = 2.8MA pulses at different He^3 concentration levels. Negative ω_ϕ is defined as in the counter-I_p direction. (Right frame) Estimated torque density profile from Pulse No: 78847 with P_{ICRH} = 1.8MW and He^3 concentration = 13%. The separatrix is at $R_{sep} \approx 3.90$m and magnetic axis at $R_0 \approx 2.97$m for all shots. Reprinted from [16,17].

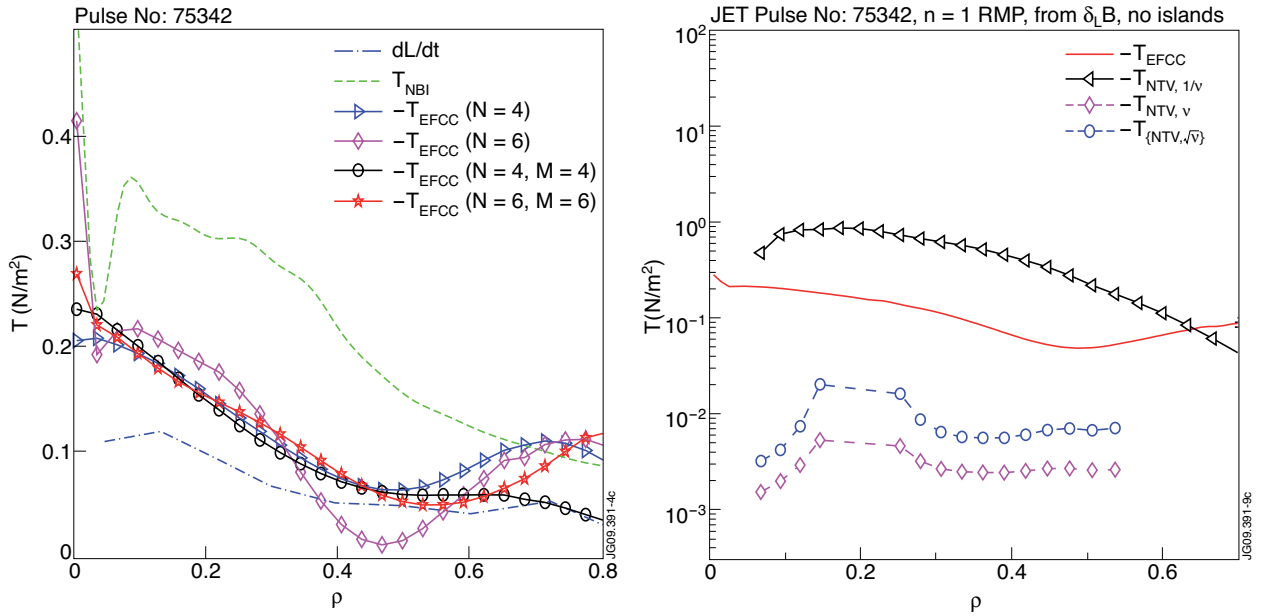

Figure 4: (Left frame) Observed TEFCC profile by using the χ_ϕ (N) and vpinch (M) profiles fitted from different orders (N = 4, M = 0 triangles, N = 6, M=0 diamonds, N = M = 4, circles, N = M = 6, pentacles) of polynomial base functions, the NBI torque (dashed line) and dL/dt (dashed dotted line) at the time just after the switch-off of the EFCC current. (Right frame) Comparison of the NTV torque profiles from the non-resonant component (resonant components assumed screened) of the perturbation field with the observed torque profile for different collisionality assumptions within the collisionless regime. Reprinted from [18].

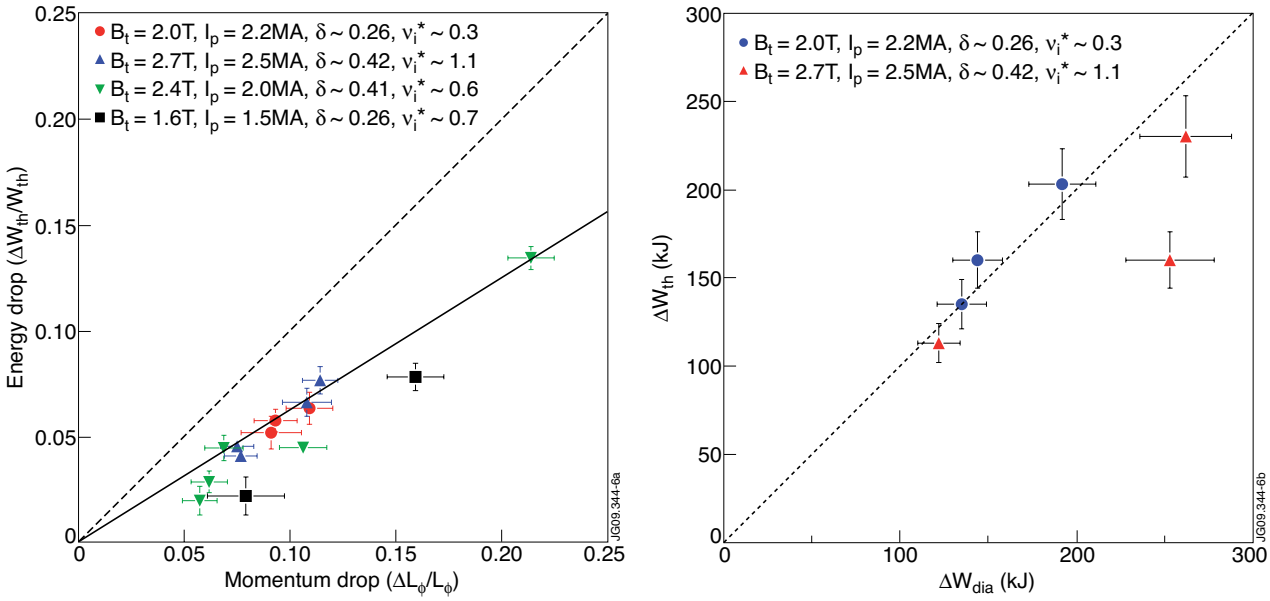

Figure 5. (Left frame) Normalised thermal energy drop versus the normalised momentum drop for several different plasma discharges under varying operating conditions. The drop in angular momentum is consistently larger as compared with the thermal energy drop by roughly a factor of 1.6 (full line). (Right frame) W_{th} (circles) and L_φ (triangles) normalised to a reference discharge without external fuelling. Open symbols refer to the charge-exchange losses L_{CX} and W_{CX} using the calibrated neutral density profile and integrated up to 95% of the plasma radius. Reprinted from [19,20].